FAILURE OF CARBON FIBER COMPOSITES WITH THERMOSET AND THERMOPLASTIC MATRIX INVESTIGATED BY IN-SITU MONITORING USING COMPUTED TOMOGRAPHY AND ACOUSTIC EMISSION

S. Kalafat[1], M.G.R. Sause[1]

[1] Institute of Physics, Experimental Physics II, University of Augsburg, 86159 Augsburg, Germany
Email: sinan.kalafat@physik.uni-augsburg.de Web Page: http://www.physik.uni-augsburg.de/exp2

Keywords: composite material, computed tomography, thermoset, thermoplastic, acoustic emission

Abstract

The objective of this study is to examine the differences in failure modes of carbon composite materials with a thermoset epoxy matrix in comparison to a thermoplastic PA6 matrix. The complex crack propagation and evolution will be described and compared. Also the influence of the matrix material on the fracture behaviour will be discussed. The fracture behaviour will be analysed using in-situ computed tomography with combined acoustic emission analysis. The load is applied with a specifically designed mechanical load stage with digital force and elongation measurement. Attached to the load stage is an acoustic waveguide which allows an undisturbed acoustic transmission path from the specimen to a broadband flat response acoustic emission sensor. The load is applied incrementally using load-hold cycles at multiple load levels to failure. During the hold period a computed tomography scan of the loaded specimen with a resolution of 1.7 µm is performed. We compare the stress-strain behaviour, the evolution of cracks and the acoustic emission release for thermoplastic and thermoset based carbon composites. Differences in the topology of the 3D crack surfaces and the influence of matrix system ductility will be discussed. Ultimately these investigations help to understand the differences in the failure mechanisms due to the ductility of the matrix material and provide a sophisticated basis for the development of more accurate failure models.

1. Introduction

The initiation and the evolution of a crack in carbon composite materials can develop along various possible paths. In a homogeneous composite it is possible that fibres and matrix fail individually or interfacial damage occurs. Furthermore, there are many factors to consider for failure analysis such as the crystallinity of the polymer matrix, the flow of the matrix or whether the state of stress is multiaxial, to highlight just a few. Current crack propagation models reach their limits in accuracy due to the variety of influencing factors governing crack propagation in a composite. This reduces the general predictability of global structural failure which on the other hand leads to higher safety margins in the design of carbon composite materials.

One of the most common simplifications in current failure prediction models is the underlying assumption of a brittle material behaviour for the matrix material. This assumption is usually only valid for composite materials which have a sufficiently cured thermoset matrix since a 3D cross-linked network of chemical bonds typically leads to brittle material failure. In contrast, carbon composite materials with a thermoplastic matrix often show a ductile material failure. In general, global structural failure in composites is the result of a complex heterogeneous evolution of different microscopic failure mechanisms. The understanding of the fundamental mechanisms is key to understand and predict global failure.

One promising approach is to use computed x-ray tomography (CT) to visualize the damage evolution in carbon composite materials before and after the final failure [1]. Such scans are also possible with an in-situ loading of the specimen within the CT [2]. In this context in-situ refers to load-hold cycles with intermediate CT scans. The advantages are that the cracks which are initiated during the test

Excerpt from ISBN 978-3-00-053387-7

are still opened and thus easier to detect. As disadvantage, especially at high stresses and longer hold periods, stress relaxation and material creep occurs. There are several groups which applied this approach to acquire a volumetric image of mechanically loaded specimens [3]–[11].

To complement our understanding of the nature of the crack initiation and propagation we extended the in-situ loading within the CT by acoustic emission testing to improve the detection and evaluation of failure. This combination yields a possibility to correlate the volumetric images (visual technique) with the acoustic emission release (acoustic technique) and the stress strain relation (mechanical technique) which are recorded throughout the observation time. Since acoustic emission events are caused during initiation and propagation of the crack it is possible to track the temporal evolution of the crack during the load and hold cycles. The current work demonstrates this approach in application to thermoplastic and thermoset based composite materials for the fundamental failure modes in tensile and compression measurements with a fibre direction perpendicular to the force axis.

2. Experimental

The combination of an in-situ mechanical testing inside of a CT with acoustic emission requires modification of current mechanical testing stage concepts to allow detection of acoustic emission signals which are free from reflexions or changes in the propagation path itself. Mechanically it is important to reach a geometrically stable load introduction and optically it is important to achieve a resolution to spot single fibre filaments (i.e. a resolution between 1µm to 3µm). Acoustically it is better to have a big specimen to have a larger volume for crack propagation and thus to detect more acoustic emission events. Also it is not possible to attach the acoustic emission sensor directly to a microscopic specimen. For CT scans, based on the shadow microscopy principle, a smaller specimen results in a higher resolution at otherwise constant parameters.

A solution for this problem is the use of a waveguide for the transfer of acoustic emission from the specimen to the sensor. Figure 1 shows the design of the entire load stage including the waveguide and the sensor placement. The slender waveguide was designed in a way that it does not show characteristic resonances or reflexions in the investigated spectrum up to 1 MHz. Also the AE sensor and the acoustic propagation path is decoupled from the other moving parts of the load stage like the motor which could otherwise cause unwanted noise-type acoustic emission signals. The dimensions of the specimens which meet the mechanical/optical and acoustic conditions are (1.9 mm × 1.7 mm) ± 0.1 mm × 2.8 mm ± 1 mm length × width × height. The specimens are cut out of the prepared laminates using a water cooled low speed saw with a diamond blade.

In one case a thermosetting matrix system (carbon epoxy prepreg laminate type Sigrafil CE1250-230-39) is used, which was produced following the curing cycle recommended by the manufacturer at 120 °C. In the other case a thermoplastic matrix material (carbon PA6 tape type CFR-TP PA6 CF60-01) was used following a heat-press cycle recommended by the manufacturer guidelines. Prior to testing the PA6 specimens were additionally stored in a vacuum oven at 80 °C to reduce moisture effects which are known to have a strong influence on the mechanical behaviour.

The prepared specimens are then adhesively bonded into steel load bars with an epoxy adhesive UHU Plus endfest 300. The mechanical test is carried out displacement controlled using a displacement rate of 0.2 mm/min. The force is recorded synchronously to the displacement by the software Microtest (Deben). The acoustic emission sensor is mechanically attached by a screw thread to the load bar which acts as a slender waveguide. During the experiment the acoustic emission is measured by a KRNBB-PC type AE sensor (KRN) with a flat frequency response in the bandwidth ranging from 1 kHz to 3 MHz and a PCI-2 data acquisition card (Mistras). The signals are preamplified using a 2/4/6 voltage switch selectable gain differential preamplifier (Mistras) at 20 dB_{AE} gain using a threshold of 39 dB_{AE}. For all configurations, an analogue bandpass filter ranging from 1 kHz to 3 MHz was used. The detection settings for the Peak-Definition-Time/Hit-Definition-Time/Hit-Lockout-Time were 10/80/300 using the software AEwin (Mistras) with a 40 MHz sampling rate. For evaluation of the corresponding failure mode, a CT scan was performed after recording an AE signal.

Excerpt from ISBN 978-3-00-053387-7

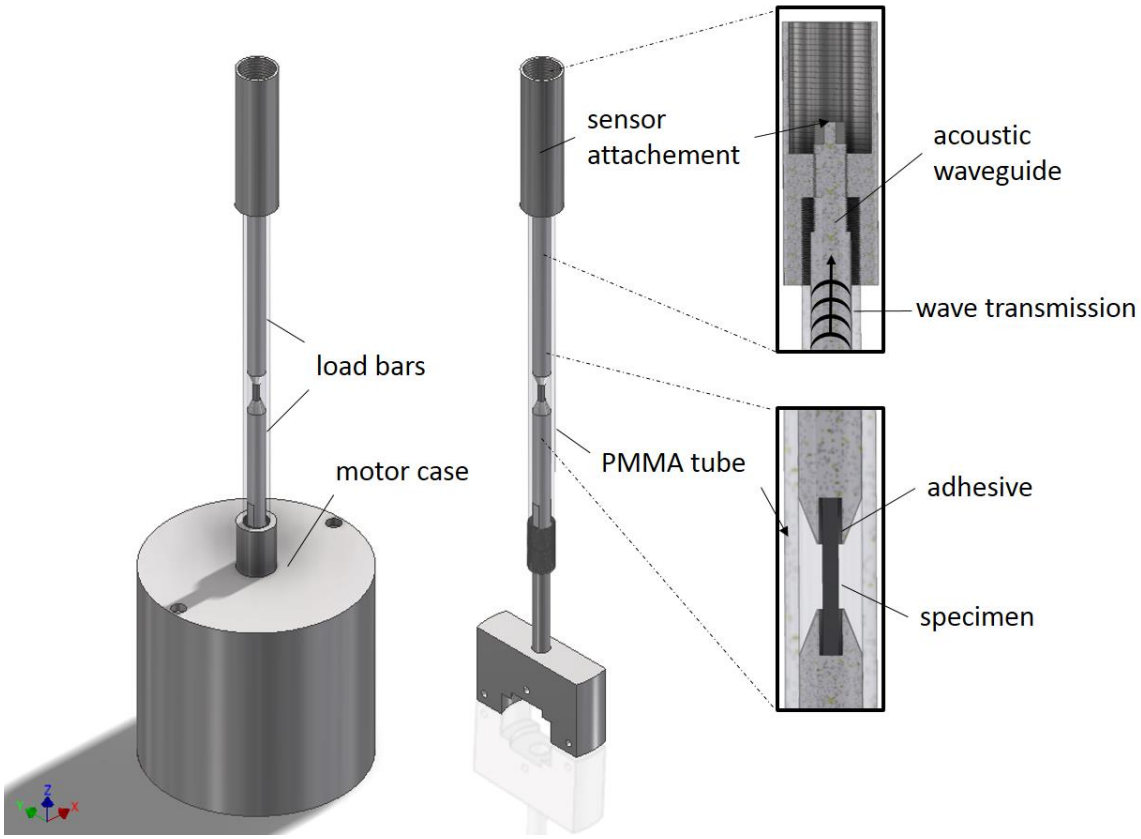

Figure 1. 3D drawing of in-situ load rig optimized for AE acquisition showing full device (left) and interior design with some parts removed (centre) as well as details of specimen and sensor attachment (right).

The CT measurements were conducted with a Nanotom m 180 (GE) which has a detector resolution of 3072 pixels x 2400 pixels. Every measurement consists of 1000 angular images with an exposure time between 1 - 2 seconds depending on the desired gray value distribution. A voltage of 50 kV with a current of 170 µA was used with a focus-object-distance and focus-detector-distance which yielded a voxel size of 1 µm to 3 µm depending on the investigated area. The three-dimensional volumes were obtained using the software phoenix datos|x2 reconstruction (GE) and post processing was done by VGStudio MAX (Volume Graphics). The chosen voxel size between 1 µm and 3 µm results in detectability of single fibres on the fracture plane as well as inclusions (e.g. pores, fire retardants) in the bulk composite.

A summary of the investigated cases in this study is given in table 1.

Table 1. Summary of the measurements with a perpendicular fibre orientation with respect to the force direction

Measurement campaign	**#1**	**#2**	**#3**	**#4**
Matrix	Thermoset (Epoxy)	Thermoplast (PA6)	Thermoset (Epoxy)	Thermoplast (PA6)
Loading condition	Tensile	Tensile	Compression	Compression

Excerpt from ISBN 978-3-00-053387-7

3. Results

In the following the results of the tensile (subchapter 3.1) and compression (subchapter 3.2) measurement campaign are briefly presented.

3.1 Tensile loading

The figure 2 shows the final results of the measurement campaign #1 and #2 with a fibre orientation perpendicular to the force direction in a tensile test as a comparison between thermoset and thermoplastic based composites. The upper part shows the thermoset based matrix system and the lower part the thermoplastic matrix system. The left side of the figure each shows the specimen and the global crack surface with the force direction. On the right side a small representative area of the crack surface is magnified. The stress-strain relation is depicted in the middle of the figure for both composite systems. Finally, the crack topology is evaluated along a cutline which is marked on the specimen. To get a quantitative approximation for the comparison of the crack branching, respectively the crack surface roughness the following formula 1 and 2 are applied.

$$R_a = \frac{1}{N}\sum_{n=1}^{N} |y(x) - \langle y(x)\rangle| \quad (1)$$

$$\langle y(x)\rangle = \frac{1}{N}\sum_{n=1}^{N} y(x) \quad (2)$$

Whereas R_a is the roughness average and N the number of samples along the cutline and y(x) is the height profile along the direction x.

For the epoxy matrix material, it can be seen that the crack surface is almost perfectly orthogonal to the force axis. The R_a roughness is around 23 µm. The specimen is separated in two pieces whereas the crack surface morphology indicates only a few fibre breaks and a smooth crack plane. In general, the epoxy matrix specimens exhibit a very brittle behaviour and indicate the crack formation and propagation is predominantly occurring in a distinct crack plane. This is noticed in the stress-strain curve as sudden load drop without visible plastic deformation and also in the acoustic emission resulting in only one acoustic event during the test.

Figure 2 on the bottom shows the thermoplastic matrix material specimen in its final stage. This is defined as the largest load drop and the final separation of the specimen in at least two pieces. It can be seen that even though the fibre orientation and the force direction is the same as in the thermosetting case the resulting failure behaviour is fundamentally different. For the particular case shown there are many additional cracks in the specimen besides the main crack. Also neither the main nor the additional cracks did propagate in a straight plane perpendicular to the force direction. The most obvious difference between the two material systems is that in the thermoplastic case there are many single fibres sticking out of the crack surface. It can be seen that the crack surface is fairly rough in comparison to the thermoset matrix material and also exhibits numerous fibre breaks. The R_a roughness is around 47 µm which is 2 times higher than the crack roughness of the epoxy based composite. Especially the single fibres indicate how the crack propagated. Parts of the fibres show extreme bending angles and the surrounding crack surface is dominated by chunks of individual fibres sticking out of the crack surface. This proves that there is not one distinguished crack plane which is initiated at one stress concentration point and then propagates throughout the entire specimen. Instead a complex evolution of multiple fibre breaks, fibre pull-outs and matrix cracks starting and interacting at spots where local stresses exceed the local strength is observed. Still crack initiation points are expected to be voids or inclusions or other imperfections of the material, but the crack propagation direction tends to deviate from preferential crack orientations such as expected from classical failure models. In the stress-strain response the curves also indicate a sudden load drop during final failure. However, the acoustic emission shows up to 1000 events being recorded during the entire test.

Excerpt from ISBN 978-3-00-053387-7

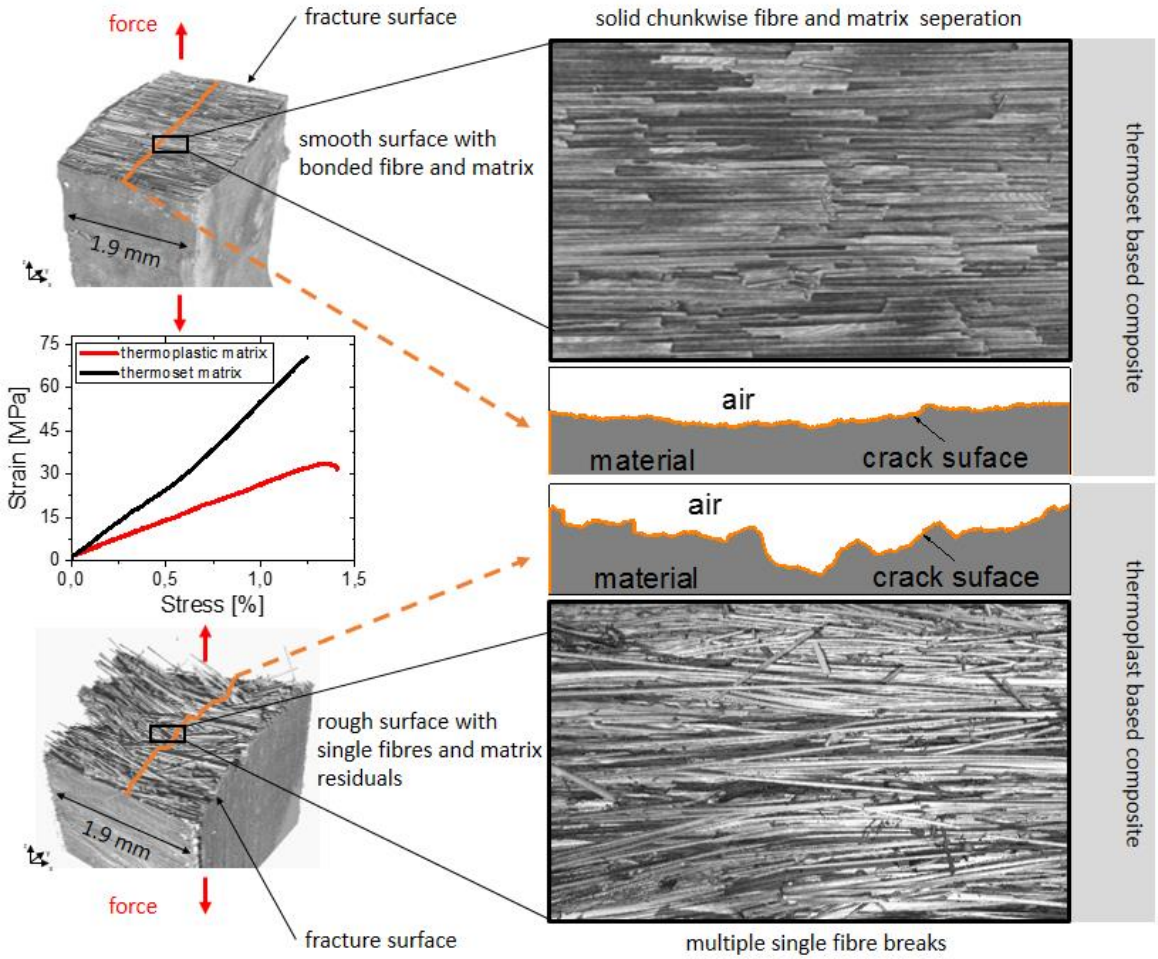

Figure 2. 3D scan of a tensile failure mode in an in-situ load rig of a thermoset and thermoplast based composite.

3.2 Compression loading

The figure 3 shows the results of the measurement campaign #3 and #4. The upper half depicts the final crack surface after compression testing of the composite system with a thermoset matrix whereas the lower half shows the thermoplastic case. On the left side the global crack surface with the principal force direction is shown with magnification of a small area on the right side of each case. Also an orange line indicates the cutline for the evaluation of the surface height profile which is determined by the formula for R_a defined in formula 1.

It can be seen that also in the case for compression the crack propagates fundamentally different for different matrix systems. The magnification represents the general behaviour on the crack surface for both cases. It is evident that the crack which separates the thermoset composite is rather smooth and has a distinct crack plane whereas the thermoplastic crack surface shows an extremely disordered rough surface area with a high amount of separated single fibres and chunks of matrix.

In the case of the PA6 matrix system the crack surface has an angle of 54.4° ± 1.3° relative to the force axis with around 600 acoustic emission signals detected, whereas the epoxy based system has an crack angle of 64.9° ± 1.1° with only 60 acoustic emission signals. The R_a value is 28 µm for the thermoset and 45 µm for the thermoplastic system.

Excerpt from ISBN 978-3-00-053387-7

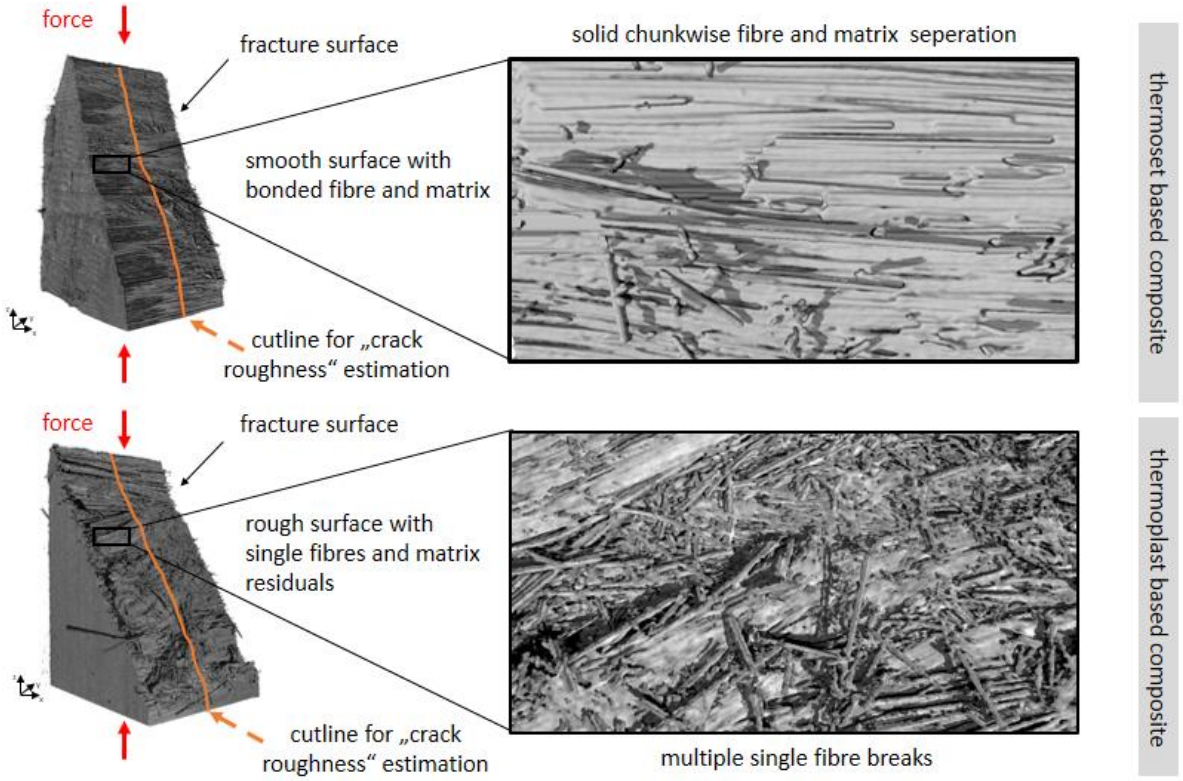

Figure 3. 3D scan of a compression failure mode in an in-situ load rig of a thermoset and thermoplast based composite.

Since the direction/angle of fibres and the force direction is identical in both test cases the change in the crack angle indicates that the principle force components within the composite change with the change of the matrix system. Especially in the case for thermoplastic materials like PA6 shear forces lead to plastic deformation due to free chain molecules being stretched locally which is not possible in thermoset materials. This local flexibility leads not only to a crack deflection but also to a rounding of the crack tip and branching of the crack path pulling out single fibres on the entire crack surface. This on the other hand is the explanation of the 10 times higher acoustic emission release from 60 (Epoxy) to 600 (PA6) signals during the test and the increased surface roughness.

4. Conclusion and Outlook

The investigated cases for thermoset and thermoplastic matrix based composites show fundamentally different behaviour of crack propagation. The volumetric CT images in combination with the acoustic emission analysis provide an insight to the nature of both failure behaviours. The three-dimensional information was used to investigate the general crack topology and the tendency of single fibre breaks or matrix cracks for the presented cases. In ongoing cases also the spatial fibre volume fraction and the porosity previous to the final crack will be investigated along with the displacement field and the local stress-strain relation. The acoustic emission also provided significant additional information for the understanding of the fundamental processes during the crack evolution. The fact that the acoustic emission density is 10 times higher for the thermoplastic case indicates a slower crack propagation with multiple fibre breaks, fibre pull-outs and matrix cracks starting and interacting at spots where local stresses exceed the local strength. In further studies additionally to pure hit detection a pattern recognition approach will be applied to distinguish between fibre/matrix and interfibre cracks. Also the relation between the crack source and the energy/amplitude which can be obtained by using the information of CT and acoustic emission can provide further insight into the nature of the crack propagation.

The examined cases help with the interpretation of the underlying processes especially with the use of acoustic emission signals and also serve as a data basis for further analysis. The combinations of all three in situ methods aid in the validation of microscopic failure models and will further help in the

Excerpt from ISBN 978-3-00-053387-7

development of macroscopic (global) failure models. To progress toward these goals it will be key to understand the formation of cracks and the corresponding acoustic emission signals in more complex damage scenarios.

Acknowledgments

We would like to thank Tobias Krones for carrying out parts of the measurements and Sascha Umbrich for specimen preparation.

References

[1] M. Stampanoni, A. Groso, A. Isenegger, G. Mikuljan, Q. Chen, A. Bertrand, S. Henein, R. Betemps, U. Frommherz, P. Böhler, D. Meister, M. Lange, R. Abela, and P. Boehler, "Trends in synchrotron-based tomographic imaging: the SLS experience," in Developments in X-Ray Tomography V, 2006, vol. 6318, p. 63180M–63180M–14.

[2] A. E. Scott, M. Mavrogordato, P. Wright, I. Sinclair, and S. M. Spearing, "In situ fibre fracture measurement in carbon-epoxy laminates using high resolution computed tomography," Compos. Sci. Technol., vol. 71, no. 12, pp. 1471–1477, 2011.

[3] A. E. Scott, M. Clinch, W. Hepples, N. Kalantzis, I. Sinclair, and S. M. Spearing, "Advanced micro-mechanical analysis of highly loaded hybrid composite structures," in ICCM 17 - 17th International Conference on Composite Materials, 2009.

[4] F. Ritschel, M. Zauner, S. J. Sanabria, M. G. R. Sause, B. R. Pinzer, a. J. Brunner, M. Stampanoni, and P. Niemz, "Damage evolution in wood: Synchrotron based micro-tomography as complementary evidence for interpreting acoustic emission behavior," Holzforschung, 2014.

[5] A. Groso, R. Abela, and M. Stampanoni, "Implementation of a fast method for high resolution phase contrast tomography," Opt. Express, 2006.

[6] A. E. Scott, W. Hepples, N. Kalantzis, P. Wright, M. N. Mavrogordato, I. Sinclair, and S. M. Spearing, "High resolution damage detection of loaded carbon/epoxy laminates using synchrotron radiation computed tomography," in 18th International conference on composite materials, 2011, pp. 1–6.

[7] E. Maire, V. Carmona, J. Courbon, and W. Ludwig, "Fast X-ray tomography and acoustic emission study of damage in metals during continuous tensile tests," Acta Mater., vol. 55, no. 20, pp. 6806–6815, 2007.

[8] A. E. Scott, I. Sinclair, S. M. Spearing, M. N. Mavrogordato, and W. Hepples, "Influence of voids on damage mechanisms in carbon/epoxy composites determined via high resolution computed tomography," Compos. Sci. Technol., vol. 90, pp. 147–153, 2014.

[9] G. Borstnar, M. N. Mavrogordato, I. Sinclair, and S. M. Spearing, "Micro - Mechanistic Analysis of in Situ Crack Growth in Toughened Carbon / Epoxy Laminates To Develop Micro - Mechanical Fracture Models," in ECCM16 - 16th European Conference on Composite Materials, 2014, no. June, pp. 22–26.

[10] R. Brault, a. Germaneau, J. C. Dupré, P. Doumalin, S. Mistou, and M. Fazzini, "In-situ Analysis of Laminated Composite Materials by X-ray Micro-Computed Tomography and Digital Volume Correlation," Exp. Mech., vol. 53, no. 7, pp. 1143–1151, 2013.

[11] A. J. Moffat, P. Wright, J. Y. Buffière, I. Sinclair, and S. M. Spearing, "Micromechanisms of damage in 0° splits in a [90/0]s composite material using synchrotron radiation computed tomography," Scr. Mater., vol. 59, no. 10, pp. 1043–1046, 2008.

[19] A. Puck and H. Schürmann, "Failure analysis of FRP laminates by means of physically based phenomenological models," Compos. Sci. Technol., vol. 62, no. 12–13 SPECIAL ISSUE, pp. 1633–1662, 2002.

[20] A. Puck and M. Mannigel, "Physically based non-linear stress-strain relations for the inter-fibre fracture analysis of FRP laminates," Compos. Sci. Technol., vol. 67, no. 9, pp. 1955–1964, 2007.

Excerpt from ISBN 978-3-00-053387-7

[21] F. Seco and A. R. Jiménez, "Modelling the Generation and Propagation of Ultrasonic Signals in Cylindrical Waveguides," in Ultrasonic Waves, Intech Open Access Publisher, 2012, pp. 1–28.

Excerpt from ISBN 978-3-00-053387-7